# Solids Fraction Measurement with a Reflective Fiber Optic Probe

***Steven M. Seachman****, Paul C. Yue, James C. Ludlow, and Lawrence J. Shadle. U.S. Department of Energy, National Energy Technology Laboratory, 3610 Collins Ferry Road, Morgantown, WV 26507*

## Abstract

A method has been developed to extract solids fraction information from a reflective fiber optic probe. The commercially available reflective fiber optic probe was designed to measure axial particle velocity (both up and down directions). However, the reflected light intensity is related to particle size and particle concentration. A light reflection model is used to relate the reflected light intensity to solids fraction. In this model we assumed that the reflected light intensity is a fixed fraction, $k_1$, of the total light intensity lost in penetration of a particle layer. Also, the solids fraction, $(1-\varepsilon)$, is related to particle concentration, $N$, in the light path by $N = k_2 (1- \varepsilon)$, where $\varepsilon$ is the void fraction. The values of $k_1$ and $k_2$ are determined from measurements made in a packed bed condition. The method allowed rapid characterization of local velocity and unambiguous solids fraction requiring only simple calibration of reflection light intensity packed beds at to determine effective number of layers and particle specific scattering.

## Introduction

Researchers at the National Energy Technology Laboratory have developed a Eulerian-Eulerian computational fluid dynamic model, MFIX, to simulate gas-solids flow in hot reacting systems common in energy conversion systems [9]. Validation of the performance of submodels within this code is essential to the improvement and ultimate acceptance of the model. Experimental data is needed on the local flow structure to confirm the implementation of drag relationships, granular temperature, and numerical techniques used in these computational fluid dynamics (CFD) codes. When using these CFD codes to simulate densely loaded transport reactor solids or void fraction is an important parameter which enters into key drag [e.g., 9, 10] and granular temperature [e.g., 6,7, 9, 10] relationships. The solids loading or solids fraction is also critical parameter in the operation of circulating fluidized bed in determining solids holdup in the bed affecting mixing or solids dispersion [8]. Traditionally, this parameter is determined through differential pressure measurement [1]. The use of this pressure differential method only gives the average value of solids fraction in the segment and this is confounded by the poorly understood contributions from wall shear.

Recently, a reflective fiber optic probe has also been calibrated to measure solids fraction [2]. The method of calibration implied that local reflected light intensity is representative of the average solids fraction of a predetermined column segment, which is valid only in a uniform solid distribution condition.

## The Empirical Model

The empirical model relates the measured local reflected light intensity to local solids fraction. The model is based on a combination of Beer-Lambert law of light transmission and simple light reflection from particle layers of a packed bed of known solids fraction. A series of measurements of reflected light from known number of particle layers are used to determine $k_1$ and $k_2$.

The intensity of a light beam coming off from the optical fibers and traverses through a particle layer is reduced according to the Beer-Lambert law. The reduction is due to both scattering and absorption by the particles and is collectively called light extinction here. The law of conservation of energy gives

$$I_0 = I_t + I_{ext} \tag{2}$$

where $I_0$ the light intensity emitting from the probe, $I_t$ is the transmitted light intensity, and $I_{ext}$ is the light extinction described above. The reflective fiber optic probe measures only a portion of the scattered light that reflected or scattered back into the probe's receiving fiber bundle and is designated by $I_r$.

We assumed the reflected light intensity, $I_r$, that the probe measures is a fixed fraction, $k_1$, of the total light intensity loss due to scattering and absorption. So we have,

$$I_r = k_1 * I_{ext} \tag{3}$$

and,

$$I_{ext} = I_0 - I_t \tag{4}$$

therefore,

$$I_r = k_1 \left( I_0 - I_t \right) \tag{5}$$

The Beer-Lambert Law that governs the light intensity, $I_t$, of a light beam traversing through a particle layer is [3]

$$I_t = I_0 e^{-\left( \frac{\pi d^2}{4} \right) Q N \ell} \tag{6}$$

where $d$ is the particle diameter, Q is the extinction coefficient, $N$ is the number concentration of particles per unit volume, and $\ell$ is the path length. This equation was used previously [4]. Strictly speaking, this equation is not applicable to our high particle loading condition because multiple light scattering would occur. In addition, the light beam emitting from our fiber optic probe is divergent. Both of these effects are not easily accounted for in the Beer-Lambert law. In our model we empirically determined the effects through equation (5). In the model, for a single particle layer with a thickness of one particle diameter the effect of multiple light scattering would be minimized and equation (6) should be applicable.

In addition, we express $N$ in equation (6) in terms of solids fraction, a parameter used by engineers and modelers in circulating fluidized bed study:

$$N = k_2 \left( 1 - \varepsilon \right) \tag{7}$$

where (1-$\varepsilon$) is the solids fraction, and $k_2$ is the conversion factor from number concentration to solid volume fraction.

Figure 1 illustrates the working principle of a three-layer model. It can easily be extended to as many layers as suitable for the sampling volume size. $I_i$ *(i =1,2,…)* is the transmitted light intensity through layer *1, 2, …,* respectively, $I_{ri}$ (*i =1,2,…*) is the reflected light intensity from layer *1, 2,…,* respectively. The factor $e^{-QN\ell}$ in equation (6) governs the light intensity attenuation for both transmitted and reflected light intensity for subsequent layers. Thus, the contribution to total reflected light intensity from each layer decreases from each additional layer and approaches a constant value.

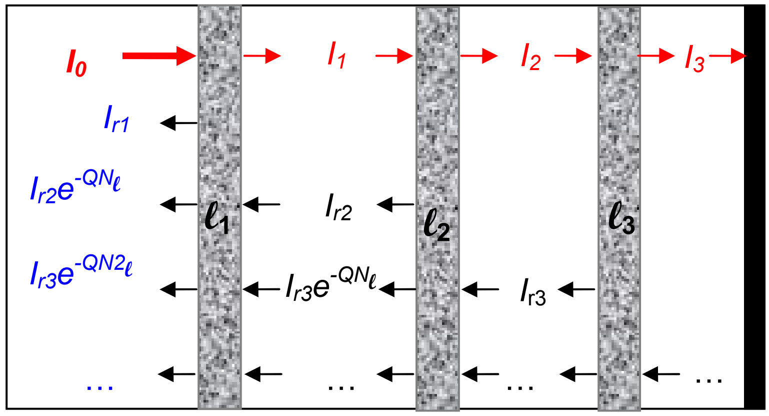

**Figure 1 - Model of Reflected Light Intensity Measurement**

With reference to the first line in **Error! Reference source not found.**, the illuminating beam intensity, $I_0$, becomes $I_1$ after penetrating the first layer, $l_1$, and becomes $I_2$ after passing through layer $l_2$, and so on. Equations 8a and 8b illustrate how $I_1$, $I_2$… etc. can all relate back to $I_0$. Equations 9a and 9b illustrate the measured reflected light intensity, $I_r$ can also relate back to $I_0$ once $k_1$ is determined.

$$I_1 = I_0 e^{-\frac{\pi d^2}{4} Q k_2 (1-\varepsilon)\ell} \quad \text{(8a)} \quad ; \qquad I_2 = I_1 e^{-\frac{\pi d^2}{4} Q k_2 (1-\varepsilon)\ell} \quad \text{(8b)}$$

$$I_{r1} = k_1 (I_0 - I_1) \quad \text{(9a)} \quad ; \qquad I_{r2} = k_1 (I_1 - I_2) \quad \text{(9b)}$$

In order to determine the appropriate number of layers, we combined equations (8) and (9) and obtained a generalized expression:

$$I_{r_{measured}} = \sum_{n=0}^{i} I_{r_{n+1}} e^{-nQk_2(1-\varepsilon)\ell} = k_1 I_0 \left[ \sum_{n=0}^{i} \left( e^{-2nQk_2(1-\varepsilon)\ell} - e^{-(2n+1)Qk_2(1-\varepsilon)\ell} \right) \right] \quad \text{(10)}$$

This is used to perform layer contribution to the total reflected light intensity analysis.

**Packed Bed Measurements to Determine $k_1$ and $k_2$.**

The values of $k_1$ and $k_2$ in our model are determined through measurements with a packed bed in which the solids fraction has been determined. The probe was placed at the top of a packed bed of particles, pointing upward, and the reflected light intensity is measured with the probe moving into the packed bed at 0.1mm increments until the reflected light intensity reached a constant value. The results of this measurement are shown in . The coefficients of the fitted curve are used to approximate the expected accumulated reflected light intensity from the particle layers used in the model to determine $k_1$ and $k_2$.

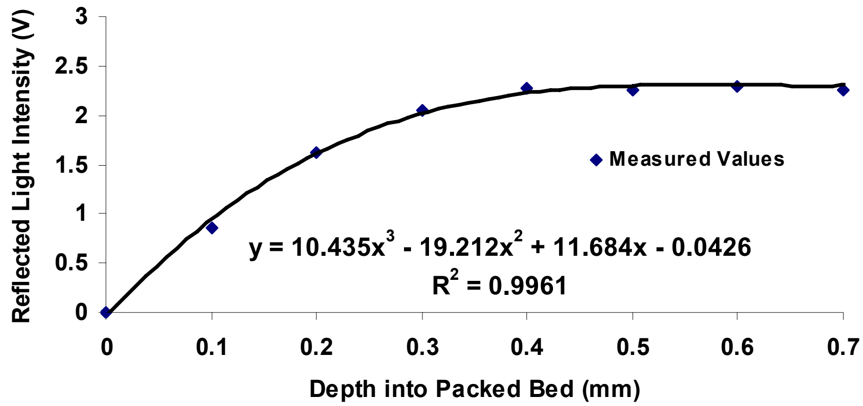


**Figure 2 - Bed Depth Measurement**

As can be seen in Figure 3, the 4 particle layer ($i$=3) agrees best with the measured data. The values calculated from these constants never had a difference higher than 4% above or below the measured values.

## Summary

The solids fractions determined by this semi-empirical technique are compared with the previous approach reported by Seachman, et al [4] and the pressure differential method. as shown in Figure 4.

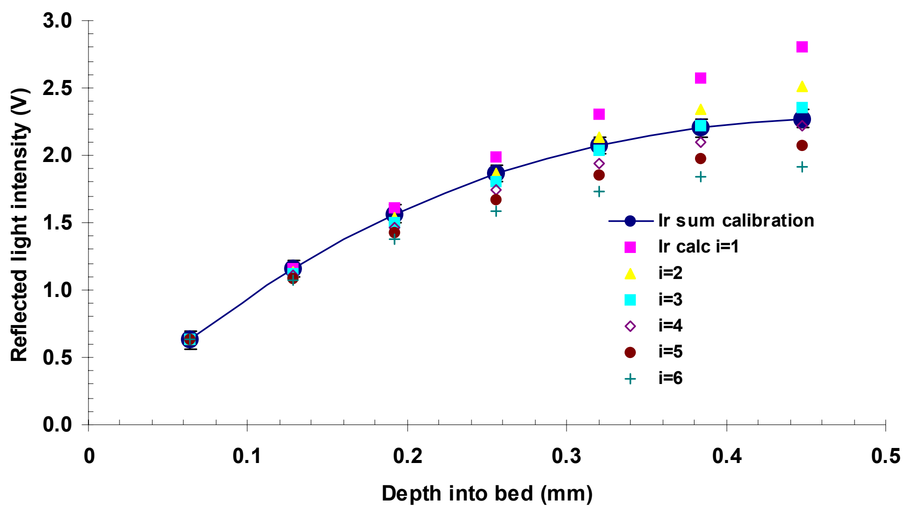


**Figure 3 - Interpolated Values Compared Against Calculated Values**

As pointed out earlier, the optical probe measures local reflected light intensity and in order to compare with the pressure differential method it is necessary to integrate the optical radial measurements to obtain the average. For this purpose optical measurements were taken at five equal area radial locations and integrated to find the average solids concentration over the riser cross section. This could either overestimate or underestimate the actual loading, depending on the radial location where the measurements are made, on the uniformity of particle distribution and on size and number of particle clusters. However, this uncertainty of solids fraction was minimized by taking measurements in the fully developed region of the CFB riser. The measurements used in Seachman et al proved statistically that the concentration in the fully developed region of the CFB riser was azimuthally independent [4]. On the other hand, solids concentrations found using pressure differential measurements depend on flow conditions. It has been reported that in core annular flow conditions the pressure differential method could underestimate the actual loading or solids fraction due to substantial downflow at the wall [5].

With reference to Figure 4, it can be seen the current technique agrees better with the pressure differential method than that used previously. At loading ratios, the ratio of solids mass to total mass of solids and gas, from 15 to 20, the new approach agrees quite well with pressure differential method. At a higher loading ratio of 34, both algorithms deviated significantly from pressure differential measurements. However, as mentioned previously, the method of finding solids concentrations through pressure differentials can underestimate the solids loading [5].

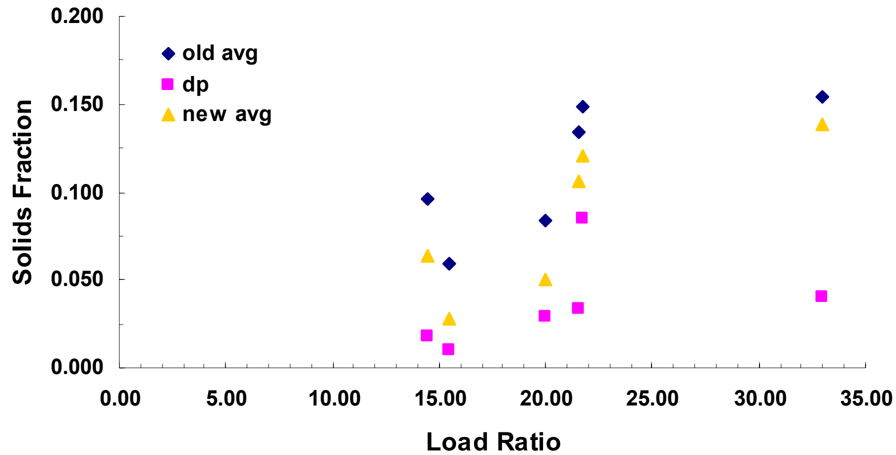


**Figure 4 - Solids Fraction Comparison**

The advantage of the current empirical technique provides us a means to better understand solid behavior in a two-phase in fluidized bed with the measurement of local solids fraction and to evaluate the uniformity of particle mass flow in a fluidized bed.

## References


[1] A. Magnusson, R. Rundqvist, A.E. Almsedt, F. Johnsson. (2005). Dual fiber optical probe measurements of solids volume fraction in a circulating fluidized bed, Powder Technology, 151, 19-26.

[2] H. Zhang, P. Johnston, J. Zhu, H. de Lasa, M. Bergougnou. (1998). A novel calibration procedure for a fiber optic solids concentration probe. Powder Technology, 100, 260-272.

[3] van de Hulst, H.C. Light Scattering by small particles. New York: Dover. P. 401

[4] S. Seachman, P. Yue, E. Taylor, L. Shadle. (2005). Solids Fractions and Flow Characteristics in a CFB as Measured with a Fiber Optic Probe. AIChE. (Ohio).

[5] J.J. Nieuwland, R. Meijer, J.A.M Kuipers, W.P.M. van Swaij, Measurements of solids concentration and axial solids velocity in gas–solid two-phase flows, Powder Technol. 87(1996.)127–139.

[6] Gidaspow D, Huilin L. "Equations of state and radial distribution functions of FCC particles in a CFB", *AIChE Journal;*1998;44(2), 279-293.

[7] Neri A, Gidaspow D. "Riser hydrodynamics: simulation using kinetic theory", *AIChE Journal,* 2000;46 (1), 52-66.

[8] Breault, R. W. "A Review of Gas-Solid Dispersion and Mass Transfer Coefficient Correlations in Circulating Fluidized Beds", *Powder Technology* 163 (2006) 9-17.

[9] Syamlal, M., Rogers, W.A., and O'Brien, T.J., (1993), MFIX Documentation and Theory Guide, DOE/METC-94/1004, NTIS DE94000087. Electronically available from: http://www.mfix.org/documentation/Theory.pdf
[10] Gidaspow, D., 1994. Multiphase Flow and Fluidization: Continuum and Kinetic Theory Description. Academic Press.